



1 **Synergistic effects of previous winter NAO and ENSO**
2 **on the spring dust activities in North China**

3 **Falei Xu¹, Shuang Wang¹, Yan Li², and Juan Feng¹**

4 ¹State Key Laboratory of Remote Sensing Science, Faculty of Geographical Science, Beijing
5 Normal University, Beijing, China

6 ²Key Laboratory for Semi-Arid Climate Change of the Ministry of Education, College of
7 Atmospheric Sciences, Lanzhou University, Lanzhou, China

8 **Correspondence:** Juan Feng (fengjuan@bnu.edu.cn)

9 **Abstract**

10 Dust plays an important role in influencing global weather and climate via impacting the Earth's
11 radiative balance. Based on the atmospheric and oceanic datasets during 1980-2022, the impacts of
12 preceding winter North Atlantic Oscillation (NAO) and El Niño-Southern Oscillation (ENSO) on
13 the following spring dust activities over North China are explored. It is found that both NAO and
14 ENSO exert significant effects in influencing the dust activities over North China, particularly
15 during their negative phases. A synergistic influence on the dust activities in North China is observed
16 when both NAO and ENSO are in negative phase, with their combined impacts exceeding that of
17 either factor alone. The previous winter NAO exhibits significant impacts on the sea surface
18 temperatures (SST) in the North Atlantic, associating with an anomalous SST tripole pattern. Owing
19 to the persistence of SST, these anomalies can extend into the following spring, when anomalous
20 atmospheric teleconnection wave trains would be induced, thereby influencing the dust activities in
21 North China. ENSO, on the one hand, directly impacts dust activities in North China by modulating
22 the circulation in the Western North Pacific (WNP). Moreover, ENSO enhances the NAO's effect
23 on the North Atlantic SST, explaining their synergistic effects on the dust activities over North China.
24 This study explains the combined role of NAO and ENSO on the dust weather over North China,
25 providing one season ahead signals for the forecast of spring dust activities in North China.

26



27 **1. Introduction**

28 Dust, as one of the most significant natural aerosols in the atmosphere, is of great importance
29 to the global radiative balance with its light-absorbing properties, exerting a crucial role in climate
30 change (e.g., Lou et al., 2017; Li et al., 2022; Kok et al., 2023). Moreover, dust not only influences
31 its source regions but also extends its impact across oceans via teleconnections driven by
32 atmospheric circulation. This transboundary transport affects ocean-atmosphere interactions and has
33 a profound impact on the Earth's climate system (Huang et al., 2015). Dust weather, resulting from
34 regional dust surges, poses a formidable threat to socio-economic development, natural ecological
35 environment, as well as human health and safety (e.g., Zhao et al., 2020; Yin et al., 2021; Li et al.,
36 2023). The Gobi Desert in East Asian, especially for the Mongolian Plateau and North China, is a
37 major source of dust (Chen et al., 2023; Hu et al., 2023), contributing approximately 70% of Asia's
38 total dust emissions (Zhang et al., 2003). Given that China is one of the countries most profoundly
39 impacted by dust disasters (Fan et al., 2018), exploring the variations in dust disasters in China is
40 of significant scientific and practical importance.

41 North China, primarily affected by dust weather, experienced over 80% of its dust events
42 during boreal spring (March-May) (Liu et al., 2022; Shao et al., 2023). In spring, besides the dust
43 source regions over China (mainly Xinjiang and Inner Mongolia), North China also exhibited high
44 dust concentrations and significant dust interannual variability (Liu et al., 2004; Ji and Fan, 2019).
45 Additionally, as a crucial center for politics, economy, and population, it is meaningful to investigate
46 the variations of spring dust weather over North China and to explore the relevant physical
47 mechanisms. Previous studies have revealed that the frequency of dust events in China exhibits
48 strong interannual and interdecadal characteristics, with a high frequency from the 1950s to 1970s,
49 a low frequency from the 1980s to 1990s, and a remarkable increase after 2000 (Zhu et al., 2008; Ji
50 and Fan, 2019). On interdecadal time scales, climate oscillations such as the Atlantic Multidecadal
51 Oscillation (AMO), Pacific Decadal Oscillation (PDO), as well as Antarctic Oscillation (AAO) can
52 influence the dust activities by affecting the climate background. For instance, the positive phase of
53 PDO is favorable for less dust weather by influencing the westerly belt, leading to weaker dust
54 activities (uplift and deposition) in the Asian region (Gong et al., 2006). The AMO plays a role in
55 affecting the global aridification process by altering the thermal properties between land and sea
56 (Huang et al., 2017). Additionally, the AAO may substantially regulate dust weather in China by
57 affecting the frequency of dust in East Asia through the interaction of meridional circulations
58 between the Northern and Southern Hemispheres (Ji and Fan, 2019).



59 On the interannual scale, a weaker East Asian winter monsoon (EAWM) is associated with
60 anomalous circulation over the Gobi and Taklamakan deserts facilitate transport of dust,
61 consequently increasing dust concentrations in China (Lou et al., 2016). The variations of the sea
62 ice coverage in the Barents Sea can significantly influence the intensity and frequency of dust
63 weather in China by influencing cyclone generation and thermal instability in North China (Fan et
64 al., 2018). The North Atlantic Oscillation (NAO) can exert a substantial influence on the spring dust
65 weather in North China by modulating the zonal wave train from the Atlantic to the Pacific at mid-
66 latitudes in the Northern Hemisphere, as well as the sea level pressure (SLP) gradient in the Tarim
67 Basin in China (Zhao et al., 2013). On the synoptic scale, the NAO exerts a vital influence on the
68 emergence and evolution of dust weather in North China, via its impact on the transport of transient
69 wave flux and modifications in atmospheric circulation (Li et al., 2023). Beyond extratropical
70 signals, tropical variabilities, such as El Niño–Southern Oscillation (ENSO), also significantly
71 modulated dust activities in China by regulating variations in large-scale circulation, precipitation,
72 and temperature over East Asia (Yang et al., 2022a; Kueh et al., 2023), as well as in Saudi Arabia
73 (Yu et al., 2015), Central Asia (Xi and Sokolik, 2015), and North America (Achakulwisut et al.,
74 2017).

75 From the aforementioned studies on the dust activities in China, it is seen that the NAO and
76 ENSO are two important factors, with a focus on their individual effects on the dust weather in
77 China. However, as one of the most significant climate variabilities in the extratropical and tropical
78 regions, respectively, the NAO and ENSO often co-occur and have complex interactions (López-
79 Parages et al., 2015). It is found that ENSO can influence the climate near the North Atlantic through
80 atmospheric forcing of the Pacific North America teleconnection (Wallace and Gutzler, 1981).
81 During the early winter of El Niño events, strong convective anomalies in the tropical Indian Ocean-
82 Western Pacific (Abid et al., 2021) and the Gulf of Mexico-Caribbean Sea (Ayarzagüena et al., 2018)
83 can trigger Rossby wave trains reaching the North Atlantic, leading to positive NAO signals, and
84 vice versa. Furthermore, the stratosphere, serving as an energy transmission channel, may also be
85 an important pathway for ENSO to influence the NAO (Jiménez-Esteve and Domeisen, 2018).
86 Moreover, observations and numerical simulations have demonstrated that NAO signal can induce
87 a Gill-Matsuno pattern in the tropical region of southern Eurasia, inducing a decadal enhancement
88 in the linkage between the East Asian summer monsoon (EASM) and ENSO (Wu et al., 2012).
89 When the NAO is in its positive phase, intensified northeasterlies are observed over tropical North
90 Atlantic, resulting in increased low-level moisture content and precipitation in the tropical North
91 Atlantic, paralleling with stronger convection and enhanced ENSO impact (Ding et al., 2023). These



92 researches highlight the connections and interactions between NAO and ENSO, underscoring the
93 necessity of considering their synergistic effects on the dust activities in North China.

94 The synergistic effect refers to the phenomenon where the combined impacts of two or more
95 factors is significantly greater than their individual role (Li et al., 2019). It is found that there are
96 synergistic effects in the impact of NAO and ENSO on the weather and climate over China. The
97 NAO can facilitate the development of the subpolar teleconnection across northern Eurasia
98 downstream, leading to anomalies in the high-pressure systems over the Ural Mountains and the
99 Sea of Okhotsk, which in turn affect the EASM (Wang et al., 2000). Meanwhile, ENSO exerts
100 significant impact on the convective activities in the central Pacific and induces alterations in the
101 equatorial circulation via the Pacific-East Asia teleconnection, further affecting the atmospheric
102 circulation and sea surface temperature (SST) in the Western North Pacific (WNP), ultimately
103 influencing the intensity of EASM (Wang et al., 2000). Therefore, the synergistic effects of these
104 factors can result in pronounced impacts on the EASM (Wu et al., 2009). During El Niño events,
105 SST in the central and eastern equatorial Pacific rises, enhancing convective activity near the equator,
106 which brings more moisture to North China and increases the likelihood of precipitation.
107 Simultaneously, the positive phase of NAO can alter the atmospheric pressure in the North Atlantic,
108 influencing the atmospheric circulation over the Eurasian continent. This interaction between NAO
109 and ENSO synergistically regulates, to some extent, the distribution of precipitation in North China
110 (Guo et al., 2012).

111 It is evident that the synergistic effects of NAO and ENSO exert significant impacts on the
112 climate in China. However, the synergistic impacts of these two factors on the dust events in North
113 China remains unclear, and the underlying mechanisms and processes are yet to be elucidated.
114 Therefore, this study will examine the synergistic effects of NAO and ENSO on the dust weather in
115 North China. Moreover, given that the impacts of winter NAO and ENSO on the climate in China
116 is more pronounced (Zuo et al., 2016; Zhang et al., 2021b), our analysis will concentrate on the
117 influence of previous winter NAO and ENSO on the following spring dust, thereby providing a
118 scientific foundation for predicting dust events in China. The structure of this paper is as follows:
119 Section 2 outlines the datasets and methods employed in this study. Section 3 presents the analysis
120 and findings. Section 4 contains the summary and discussion.

121

122



123 2. Datasets and methods

124 2.1 Datasets

125 The dust dataset for the Modern-Era Retrospective Analysis for Research and Applications
126 Version 2 (MERRA-2) was obtained from NASA's Global Modeling and Assimilation Office
127 (GMAO), incorporating assimilated observations from both satellites and ground stations (Gelaro
128 et al., 2017). In this study, the Dust Column Mass Density of the MERRA-2 `avg1_2d_aer_Nx`
129 product was utilized to represent the dust concentration with $0.5^\circ \times 0.625^\circ$ resolution. Additionally,
130 the SST dataset was derived from the Hadley Centre of the UK Met Office on a $1^\circ \times 1^\circ$ grid (Rayner
131 et al., 2003). The atmospheric reanalysis datasets employed herein were provided from the Fifth
132 Generation Reanalysis Version 5 (ERA5) of the European Centre for Medium-Range Weather
133 Forecasts (ECMWF) with a resolution of $0.25^\circ \times 0.25^\circ$ on 37 vertical levels (Hersbach et al., 2020),
134 including wind, geopotential height, and sea-level pressure. Considering the available period of all
135 datasets, the common available period of 1979–2022 was selected. The winter is defined as
136 December-February (December-January-February, DJF), with the winter of 1979 corresponding to
137 the average of December in 1979, January and February in 1980. The spring season is delineated as
138 the average of March-May (March-April-May, MAM).

139 2.2 Methods

140 The NAO index (NAOI) used is following Li and Wang (2003), quantified by the difference in
141 the normalized monthly SLP regionally zonal averaged over the North Atlantic within 80°W - 30°E
142 between 35°N and 65°N . This definition effectively captures the large-scale circulation
143 characteristics associated with NAO, essentially measuring the intensity of zonal winds spanning
144 the entire North Atlantic. Furthermore, ENSO is characterized by Niño3.4 index with SST
145 anomalies averaged over 5°S - 5°N , 170°W - 120°W (Trenberth, 1997). In this study, we utilized the
146 standardized indices of seasonal averages during 1980-2022, with values exceeding 0.5 standard
147 deviations identified as anomalous years as shown in Table 1.

148 The memory effect of SST can be elucidated by the SST persistence component (SST_p), as
149 delineated in equation (1) (Pan, 2005).

$$150 \quad SST_p = SST(t) * \frac{Cov[SST(t), SST(t+1)]}{Var[SST(t)]} \quad (1)$$

151 SST_p represents the memory effect of the previous SST (previous winter) on the following SST
152 (spring), where $SST(t)$ and $SST(t+1)$ denote the previous winter SST and spring SST,



153 respectively. $Cov[SST(t), SST(t + 1)]$ denotes the covariance between the previous winter SST
 154 and spring SST, while $Var[SST(t)]$ signifies the variance of the previous winter SST.
 155 Consequently, the $Cov[SST(t), SST(t + 1)]/Var[SST(t)]$ represents the connection between the
 156 SST variations in previous winter and spring. A greater value of SST_p indicates the variation of
 157 $SST(t + 1)$ is more closely attached with the variation of $SST(t)$.

158 The T-N wave activity flux (WAF), formulated by Takaya and Nakamura (2001), represents a
 159 three-dimensional wave action flux that describes the energy dispersion characteristics of stationary
 160 Rossby waves, thereby reflecting the direction of Rossby wave energy dispersion. The WAF is
 161 suitable for application in mid-high latitude regions where the background circulation deviates from
 162 uniform zonality, as obviates the need for the assumption that the basic flow field must be a zonally
 163 averaged basic flow and can accommodate zonally non-uniform wind fields. The convergence and
 164 divergence characteristics of WAF reveal the source and dissipation areas of wave energy, with the
 165 transmission direction being interpretable as the direction of energy transport. The three-
 166 dimensional formulation of WAF is as follows:

$$167 \quad W = \frac{pcos\varphi}{2|U|} \cdot \begin{pmatrix} \frac{U}{a^2cos^2\varphi} \left[\left(\frac{\partial\psi'}{\partial\lambda} \right)^2 - \psi' \frac{\partial^2\psi'}{\partial\lambda^2} \right] + \frac{V}{a^2cos\varphi} \left[\frac{\partial\psi'}{\partial\lambda} \frac{\partial\psi'}{\partial\varphi} - \psi' \frac{\partial^2\psi'}{\partial\lambda\partial\varphi} \right] \\ \frac{U}{a^2cos\varphi} \left[\frac{\partial\psi'}{\partial\lambda} \frac{\partial\psi'}{\partial\varphi} - \psi' \frac{\partial^2\psi'}{\partial\lambda\partial\varphi} \right] + \frac{V}{a^2} \left[\left(\frac{\partial\psi'}{\partial\varphi} \right)^2 - \psi' \frac{\partial^2\psi'}{\partial\varphi^2} \right] \\ \frac{f_0^2}{N^2} \left\{ \frac{U}{acos\varphi} \left[\frac{\partial\psi'}{\partial\lambda} \frac{\partial\psi'}{\partial z} - \psi' \frac{\partial^2\psi'}{\partial\lambda\partial z} \right] + \frac{V}{a} \left[\frac{\partial\psi'}{\partial\varphi} \frac{\partial\psi'}{\partial z} - \psi' \frac{\partial^2\psi'}{\partial\varphi\partial z} \right] \right\} \end{pmatrix} \quad (2)$$

168 In the expression, p , φ , λ , f_0 , and a represent the geopotential height, latitude, longitude,
 169 coriolis parameter, and Earth's radius, respectively. $\psi' = \Phi'/f$ (where Φ represents the
 170 geopotential) denotes the disturbance of the quasi-geostrophic stream function relative to the
 171 climatology. The basic flow field $\mathbf{U} = (U, V)$ denotes the climatic field, where U and V indicate
 172 the zonal and meridional velocities, respectively.

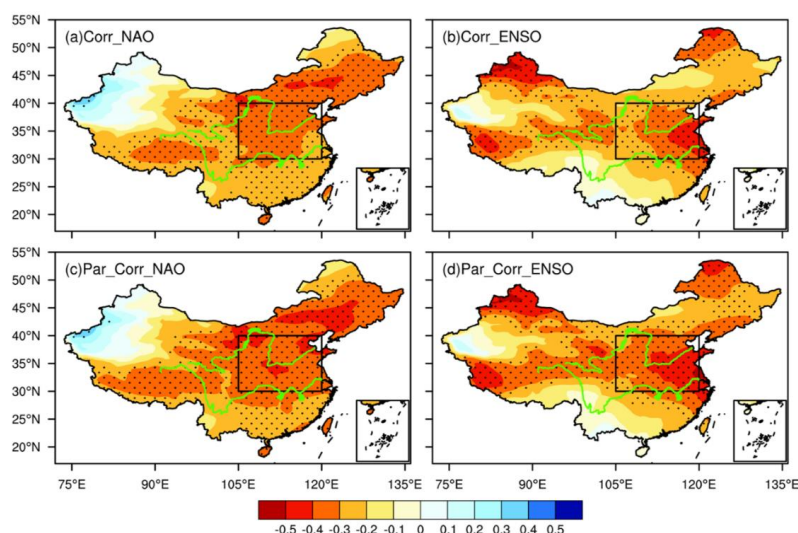
173 3. Results

174 3.1 Impacts of NAO and ENSO on the spring dust in North China

175 Previous studies have highlighted the significant impacts of NAO (e.g., Wu et al., 2009; Zheng
 176 et al., 2016a; Wang et al., 2018) and ENSO (e.g., Zhao et al., 2016; Zhang et al., 2016; Feng et al.,
 177 2020) on the climate anomalies over China. To investigate their effects on the spring dust, the
 178 correlation between the previous winter NAO and ENSO and following spring dust concentrations
 179 are examined (Figure 1). Significant negative correlations are observed over North China between



180 NAO and dust content. Similar relationship is seen in the ENSO case. This result indicates a lower
 181 (higher) dust content is expected when NAO and ENSO are in the positive (negative) phases
 182 (Figures 1a-b). Notably, North China is situated at the center of the maximum correlation.
 183 Simultaneously, considering the significant interaction between NAO and ENSO (López-Parages et
 184 al., 2015; Zhang et al., 2015), to detect their independent effects on the dust content, the partial
 185 correlation between NAO (ENSO) and dust content after removing the influence of the ENSO
 186 (NAO) are provided. The results indicate that the significant correlation regions between dust
 187 concentrations and either NAO or ENSO do not change significantly after removing the influence
 188 of the other. These findings suggest a stable and significant connection between NAO and ENSO in
 189 the previous winter and the dust content in North China (Figures 1c-d).



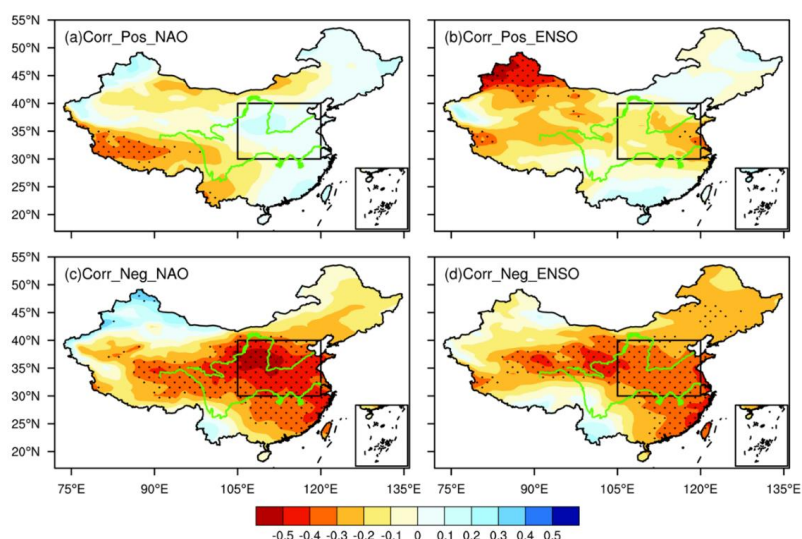
190

191 **Figure 1.** (a) Spatial distribution of correlation coefficients between the previous winter NAOI and
 192 spring dust content. (b) As in (a), but with Niño3.4 index. (c) As in (a), but for the partial correlation
 193 after removing the effect of ENSO. (d) As in (c), but after removing the effect of NAO. The black
 194 box represents North China. Stippled areas are statistically significant at the 0.1 level.

195 Previous studies have indicated that the development rate, intensity variations, and spatial
 196 structure of NAO exhibit distinct asymmetric characteristics between different phases (e.g.,
 197 Feldstein, 2003; Jia et al., 2007). Furthermore, the influence of NAO on the EAWM is more
 198 pronounced during its negative phase (Sung et al., 2010). Similarly, both observational facts and
 199 model experiments suggest that El Niño and La Niña, as the positive and negative phases of ENSO,
 200 are not simply mirror images of each other. The SST anomalies in the tropical Pacific associated



201 with ENSO exhibit significant asymmetry in terms of meridional range (Zhang et al., 2009),
202 amplitude (Su et al., 2010), zonal propagation (McPhaden and Zhang, 2009), as well as climate
203 impact (Feng and Li, 2011; Yang et al., 2022b) under El Niño and La Niña conditions. Consequently,
204 we further analyzed the connection between NAO/ENSO and spring dust but in different phases.
205 The results indicate that the relationship between NAO/ENSO and dust in North China also exhibits
206 significant asymmetry, i.e., with weaker (stronger) correlations during positive (negative) phases of
207 NAO and ENSO (Figure 2), where significant correlations only appear in the negative phases of
208 NAO and ENSO. To comprehensively understand the effects of both NAO and ENSO on the dust
209 activities in North China, the areal average of spring dust content over North China was calculated,
210 termed as the spring dust index (SDI). Based on the scatter distribution of SDI under different phases
211 of NAO and ENSO, it is noted that the correlation coefficients between NAOI and SDI during the
212 positive and negative phases of NAO are -0.46 and -0.05, respectively, indicating that the significant
213 influence of NAO on the dust in North China mainly occurs during its negative phase (Figure 3a).
214 Similarly, the correlation distribution between the ENSO and SDI also shows that the influence of
215 ENSO is more pronounced during its negative phase (Figure 3b). These results indicate that the
216 impacts of previous winter NAO and ENSO on the spring dust content in North China exhibit
217 asymmetrical characteristics, significant effects mainly manifested during their negative phases.

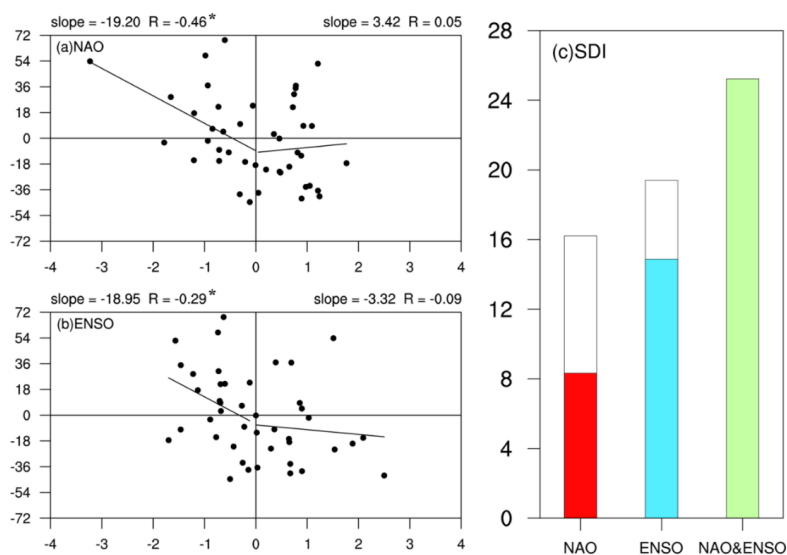


218

219 **Figure 2.** Spatial distribution of correlation coefficients between (a) positive and (c) negative NAOI
220 values and dust content. (b) and (d) As in (a) and (b), respectively, but for the Niño3.4 index.
221 Stippled areas are statistically significant at the 0.2 level.



222 The synergistic effects of climate variabilities from mid-high latitudes and tropics are pivotal
 223 mechanisms affecting the weather and climate in East Asia (e.g., Feng et al., 2019; Li et al., 2019).
 224 Correspondingly, we will examine whether the negative phases of previous winter NAO and ENSO
 225 exert synergistic effects on the following spring dust content in North China. As shown in Figure
 226 3c, when the NAO is in its negative phase, including alone occurrence and in conjunction with
 227 negative phase of ENSO, the anomalous values of dust content is $8.32 \text{ mg}\cdot\text{m}^{-2}$ and $16.21 \text{ mg}\cdot\text{m}^{-2}$,
 228 respectively. Similarly, the anomalous dust content is $14.88 \text{ mg}\cdot\text{m}^{-2}$ and $19.40 \text{ mg}\cdot\text{m}^{-2}$ for the case
 229 of ENSO. When the NAO and ENSO both are in negative phases, the value of dust anomaly (25.23
 230 $\text{mg}\cdot\text{m}^{-2}$) is much greater than the situation when one of them is in the negative phase. That is the
 231 negative phases of previous winter NAO and ENSO demonstrate synergistic effects on the spring
 232 dust activities in North China. Therefore, three categories, i.e., only the NAO (ENSO) is in its
 233 negative phase, and both NAO and ENSO are in the negative phases (Table 1) are discussed in the
 234 context to elucidate the relevant process of the synergistic effects of NAO and ENSO on the dust
 235 content over North China.



236

237 **Figure 3.** Scatterplots of the spring dust content in North China against previous winter (a) NAOI
 238 and (b) Niño3.4 index. Also shown are lines of best fit for positive and negative NAO/Niño3.4 index
 239 values and correlation coefficients (R), slope (slope), * indicates significant at the 0.2 level. (c)
 240 Spring dust content over North China during the negative NAO, negative ENSO phases, and
 241 concurrent negative phases of NAO and ENSO (unit: $\text{mg}\cdot\text{m}^{-2}$). Transparent bars represent negative
 242 phases of the NAO and ENSO, filled bars indicate negative phases of the NAO and ENSO occurring
 243 separately.



244 **Table 1.** The events of NAO and ENSO classified by three categories during period 1980-2022

	Years	Numbers
NAO	1980,1982,1985,1986,1987,1996,1998,2001, 2003,2004,2006,2010,2011,2013,2021	15
ENSO	1984,1985,1986,1989,1996,1999,2000,2001, 2006,2008,2009,2011,2012,2018,2021,2022	16
NAO & ENSO	1985,1986,1996,2001,2006,2011,2021	7

245 **3.2 Impacts of NAO and ENSO on the environmental variables**

246 To examine the anomalous characteristics associated with NAO and ENSO, the circulation
247 anomalies in their solo negative phases, as well as in their co-occur negative phases (Table 1) are
248 analyzed. In the upper troposphere (200 hPa), the zonal wind is strengthened over the northwest of
249 China and Mongolia during the negative NAO phase (Figure 4a), with evident positive anomalies
250 centered around Mongolia, reaching a maximum value of $+1.5 \text{ m}\cdot\text{s}^{-1}$. In the case of negative ENSO
251 phase, the upper-level zonal wind also shows an intensification over the northwest region of China
252 and Mongolia, with a maximum value of $+2 \text{ m}\cdot\text{s}^{-1}$ (Figure 4d). The intensification of upper-level
253 zonal wind boosts the upper-level momentum, which is subsequently transferred downward to the
254 mid-lower troposphere through vertical circulation (Wu et al., 2016; Li et al., 2023), causing windy
255 weather in the surface dust source regions, facilitating dust lifting and transport activities, thereby
256 promoting the occurrence of dust weather in the downstream North China. When both the NAO and
257 ENSO are in their negative phases, the main positive anomaly center appears over North China,
258 reaching a maximum value of $+3 \text{ m}\cdot\text{s}^{-1}$, which is stronger than the situation in either the NAO or
259 ENSO. This result implies the synergistic effects of NAO and ENSO on the upper-level zonal wind,
260 facilitating an enhanced transport of dust from its source regions to North China, consequently
261 triggering the onset of dust weather conditions in North China (Figure 4g).

262 Subsequent analysis delved into the anomalous distribution of the circulation field in the mid
263 and lower troposphere. In the negative NAO phase, a pronounced 'trough-ridge' anomaly pattern
264 emerges in the mid-latitude region, characterized by a trough in Siberia and a ridge in the Middle
265 East, with their anomalous intensities reaching -12 gpm and $+10 \text{ gpm}$, respectively (Figure 4b). This
266 atmospheric configuration fosters a dominant meridional circulation in the mid-high latitude region,
267 thereby facilitating the enhanced transport of cold air from the north. Such a southward incursion
268 of cold air serves to strengthen the surface wind speeds, and promote the uplift and transport of dust
269 from the source regions. In the negative ENSO phase, although the mid-latitude region exhibits a
270 similar trough-ridge pattern, more pronounced circulation anomalies are observed over the WNP.



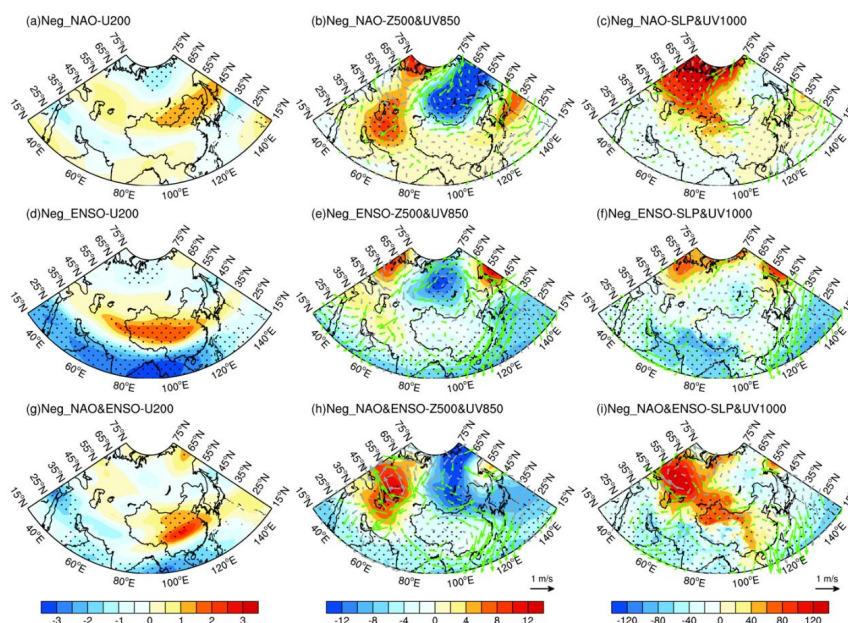
271 At this time, the region is predominantly under the influence of northeasterly winds on its western
272 flank, manifesting a cyclonic circulation anomaly (Figure 4e), consistent with previous research
273 results (Ke et al., 2023). This abnormal circulation will hinder the northward transport of warm and
274 moist air from the South China Sea and the Bay of Bengal, diminishing the likelihood of interactions
275 with cold air from the north, thus reducing the possibility for the formation of stationary fronts and
276 precipitation. The decrease in precipitation weakens the wet deposition effect (Zheng et al., 2016b;
277 Huang et al., 2021), favoring the occurrence of dust weather in the region. When both the NAO and
278 ENSO are simultaneously in their negative phases, the meridional circulation in the mid-latitude
279 region is notably enhanced, with the maximum anomalies of the trough and ridge reaching -12 gpm
280 and +12 gpm, respectively (Figure 4h). Furthermore, the southward shift of the trough-ridge pattern
281 leads to a more significant increase in wind speed in the upstream dust source regions of North
282 China, providing a more substantial source of dust for North China. Meanwhile, the presence of a
283 cyclonic circulation anomaly over the WNP reduces the transport of warm and moist air from the
284 south, which is unfavorable for precipitation, thereby lowering the wet deposition effect on dust and
285 further favoring the onset and intensification of dust activities in North China.

286 As for the SLP, significant positive SLP anomalies appear in Eastern Europe and the Russian
287 during negative NAO phase, indicative of an intensified Siberian High (SH), which extends
288 southward to the dust source regions upstream of North China (Figure 4c). The intensification of
289 the SH typically accompanied with strong northerlies and dry conditions, favoring for the transport
290 of dust, thereby supplying abundant material sources for dust activities in North China. In the
291 negative ENSO phase, although the high-latitude region exhibits a weaker SH signal, similar to the
292 ENSO influence on the circulation pattern in the middle and lower troposphere, more significant
293 circulation anomalies occur over the WNP. This cyclonic circulation anomaly inhibits the northward
294 transport of warm and moist air from the south, leading to poorer precipitation conditions in North
295 China (Figure 4f). When both the NAO and ENSO are in their negative phases, the strength and
296 influence extent of the SH are more pronounced compared to that when the NAO sole is in negative
297 phase. Besides, there persists a cyclonic circulation anomaly over the WNP, which is conducive to
298 the occurrence of dust events in North China (Figure 4i).

299 The results suggest that when both the NAO and ENSO are in their negative phases, synergistic
300 effects emerges, rendering the atmospheric circulation in the troposphere more conducive to the
301 occurrence of dust events in North China. The synergistic effects may be due to the superposition
302 and interaction of various atmospheric levels and regional characteristics modulated by the NAO



303 and ENSO, thereby forming more favorable circulation conditions for dust activities in North China.

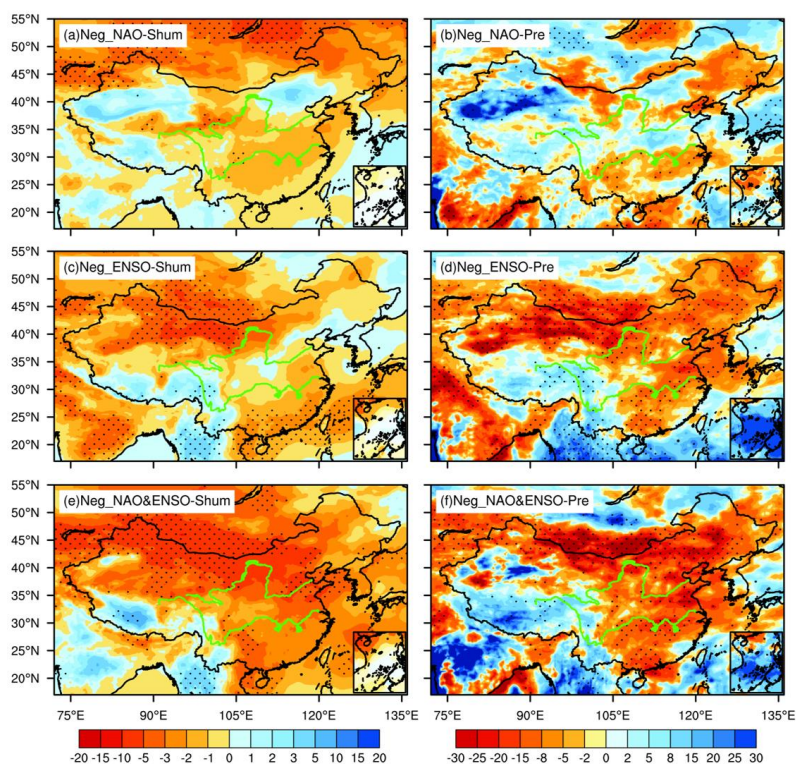


304
 305 **Figure 4.** Upper, (a) 200 hPa zonal wind anomalies (shading, unit: $\text{m}\cdot\text{s}^{-1}$), (b) 500 hPa geopotential
 306 height (shading, unit: gpm) and 850 hPa wind field anomalies (arrows, unit: $\text{m}\cdot\text{s}^{-1}$), (c) sea-level
 307 pressure (shading, unit: Pa) and 1000 hPa wind field anomalies (arrows, unit: $\text{m}\cdot\text{s}^{-1}$) during the
 308 negative NAO phases. Middle-Lower, as in the upper, but during the negative ENSO phases and
 309 concurrent negative phases of NAO and ENSO, respectively. Stippled areas and green arrows are
 310 statistically significant at the 0.2 level.

311 Dust activities are multifaceted phenomenon related to large-scale circulation patterns, and
 312 significantly influenced by local surface conditions and meteorological processes. It is found that
 313 surface properties and local meteorological factors play a role in the initiation, development, and
 314 dissipation of dust activities (e.g., Liu et al., 2004; Yao et al., 2021; Huang et al., 2021). In particular,
 315 humidity and precipitation play decisive role in determining the frequency and intensity of dust
 316 activities (Prospero et al., 1987; Kim and Choi, 2015). Low humidity leads to drier soil conditions
 317 in the dust source regions, reducing the cohesion between soil particles and facilitating dust lifting
 318 and transport activities (Csavina et al., 2014), and vice versa. Similarly, the amount of precipitation
 319 directly affects the wet deposition process of dust. Low precipitation weakens the wet deposition,
 320 resulting in relatively stronger dust activities (Zheng et al., 2016b). Therefore, we further analyzed
 321 their potential impacts on the humidity and precipitation. When the NAO is in its negative phase,
 322 humidity in the spring dust source regions and North China generally reduced, particularly in areas
 323 near the dust source regions, indicating that these areas are conducive to dust transport and prone to



324 causing dust weather in North China (Figure 5a). As for the precipitation, there is more spring
325 precipitation in the northwest region of China, while precipitation in the Mongolia and the North
326 China is relatively less (Figure 5b). In the negative ENSO phase, the variation in humidity is similar
327 to that during the negative NAO phase, but with a greater amplitude (Figure 5c), indicating that
328 ENSO has a stronger impact on the humidity conditions in North China. Moreover, the precipitation
329 shows a significant abnormal decrease over Mongolia and North China, which is highly conducive
330 to dust activities and the generation of dust weather (Figure 5d). When both the NAO and ENSO
331 are in the negative phases, the humidity anomalies in the dust source regions and North China are
332 more intense than the individual factor (Figure 5e). The variation in precipitation are similar to those
333 in humidity, the reduction in precipitation in the dust source regions and North China exceeds the
334 sole role (Figure 5f). The aforementioned analysis indicates that NAO and ENSO can modulate
335 humidity and precipitation, ultimately affecting dust weather. During the negative NAO phase, the
336 diminished atmospheric pressure gradient in the mid-high latitude regions of North Atlantic leads
337 to the intensification and southward shift of the SH (Zhou et al., 2023), accompanied by strong wind,
338 making drier and conducive to dust lifting and transport in the dust source regions. In the negative
339 ENSO phase, the upper atmosphere over the WNP is dominated by significant negative anomalies
340 in geopotential height and northeasterly winds (Zhang et al., 2015), reducing moist transport. When
341 the NAO and ENSO both are in negative phases, their regulation of atmospheric circulation
342 produces synergistic effects, further influencing the variations of humidity and precipitation, thereby
343 promoting the occurrence and development of dust activities in North China.



344

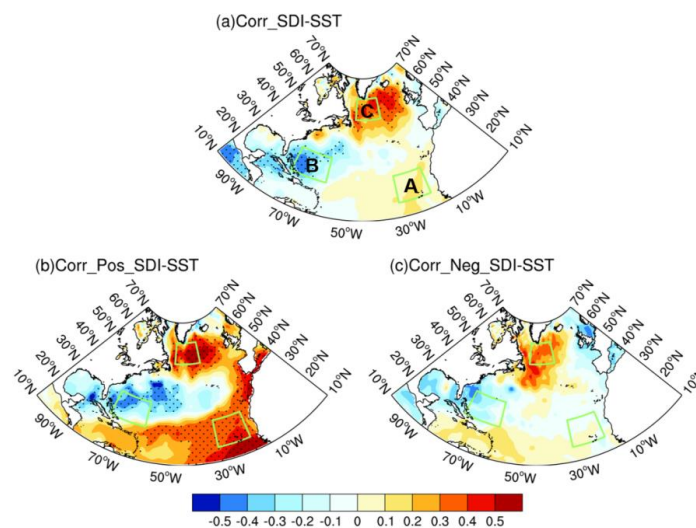
345 **Figure 5.** Upper, composite percentage anomalies of (a) humidity and (b) precipitation during
 346 negative NAO phases. Middle-Lower, as in the upper, but during negative ENSO phases and
 347 concurrent negative phases of NAO and ENSO, respectively. Stippled areas are statistically
 348 significant at the 0.2 level.

349 3.3 Physical Mechanisms of the NAO and ENSO on the dust weather

350 The above results demonstrated that the previous winter NAO and ENSO exert significant
 351 impacts on the spring dust activities in North China. Consequently, an examination of the underlying
 352 physical mechanisms is warranted. Given the relatively short memory of NAO as an atmospheric
 353 phenomenon, we will employ the concept of ocean-atmosphere coupling bridge to elucidate the
 354 involved processes. The previous ENSO signal can alter the atmospheric circulation over the WNP
 355 through the persistent impact of SST, thereby significantly affecting subsequent weather and climate
 356 in China (e.g., Wu et al., 2017; Kim and Kug, 2018; Jiang et al., 2019). The tripole configuration of
 357 SST is the leading mode of SST variation in the North Atlantic, and its variabilities are closely
 358 associated with the NAO (Czaja and Frankignoul, 2002; Wu et al., 2009; Figure 7a), which allows
 359 the previous NAO signal to exert a long-term influence on the subsequent weather and climate in



360 China (e.g., Wu et al., 2012; Zhang et al., 2021a; Li et al., 2023). The variation of SDI is linked with
 361 an anomalous tripole SST in the North Atlantic (Figure 6a), paralleling with the SST anomalies
 362 accompanied with the negative phase of NAO. Therefore, the North Atlantic tripole index (NATI)
 363 is further delineated (Equations 3-6), as well as the relationships among the NAOI, NATI, and SDI
 364 are explored. The correlation analysis between the high and low years of SDI and NATI reveals a
 365 pronounced difference, indicating an asymmetric correlation (Figures 6b-c). Specifically, the
 366 significant relationship between SDI and NATI only existed in the positive SDI years, implying the
 367 occurrence of NATI would be connected with more dust weather over North China.



368

369 **Figure 6.** (a) Spatial distribution of the correlation coefficients between the spring SDI and
 370 simultaneous SST. (b)-(c) As in (a), but for the positive and negative phase of SDI. Stippled areas
 371 are statistically significant at the 0.2 level.

372
$$SST_A = [15-25^{\circ}N, 32-20^{\circ}W] \quad (3)$$

373
$$SST_B = [22-32^{\circ}N, 75-60^{\circ}W] \quad (4)$$

374
$$SST_C = [50-60^{\circ}N, 50-32^{\circ}W] \quad (5)$$

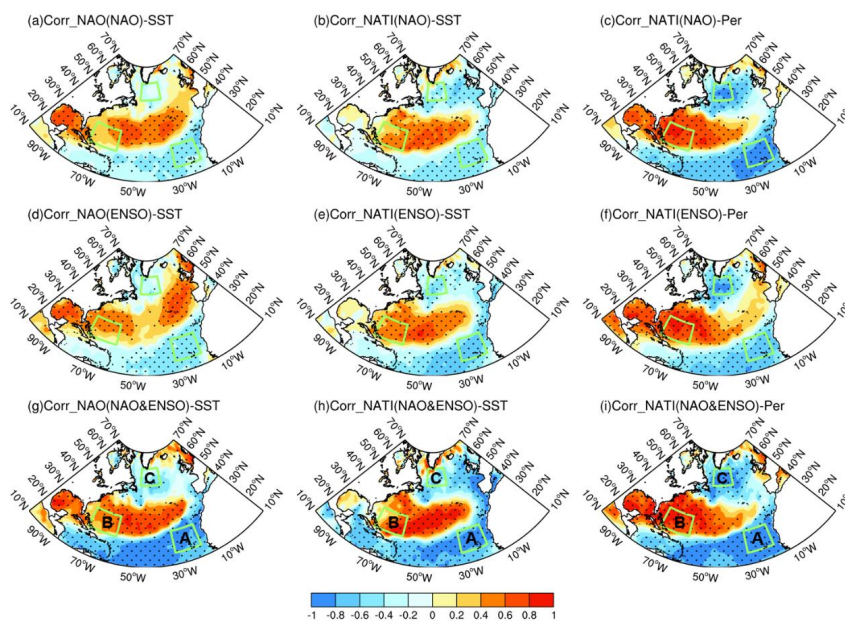
375
$$NATI = SST_B - \frac{1}{2}(SST_A + SST_C) \quad (6)$$

376 Subsequent analyses delved into the association between the previous winter NAO and the
 377 North Atlantic SST. It is seen that the correlation coefficients between the negative (positive) NAOI
 378 and NATI are 0.41(-0.09) (figures not shown), indicating that the influence of previous winter NAO
 379 on the following spring NATI only manifest during its negative phase. This elucidates the reason
 380 why the significant impact of NAO on the dust activities in North China only existed during its
 381 negative phase. In the negative NAO phase, there is a notable correlation between the previous



382 winter NATI and the spring SST and SST_p (Figures 7b-c), indicating that the previous winter NATI
 383 can persist to spring, in which the self-persistence of SST playing a crucial role. Similar findings
 384 are observed during the negative phase of ENSO (Figures 7d-f) and when both the NAO and ENSO
 385 occur simultaneously (Figures 7g-i).

386 The correlation between the previous winter NAO and North Atlantic SST reveals that in the
 387 NAO negative phase (Figure 7a), the variation of NAO is linked with an anomalous tripole SST
 388 pattern in the North Atlantic. Meanwhile, similar findings are observed when negative ENSO events
 389 occur (Figure 7d). This suggests that there may be a positive feedback occurred between NAO and
 390 North Atlantic SST during negative ENSO phase. When both the NAO and ENSO are in the
 391 negative phases, the anomalous tripole SST pattern is more pronounced (Figure 7g). This further
 392 elucidates that ENSO exerts a promoting effect on strengthening the connection between the
 393 negative NAO and NATI, thereby providing an explanation for the synergistic effects of the NAO
 394 and ENSO on the dust weather in North China. Additionally, the correlation coefficients between
 395 the NAOI and NATI under different scenarios can illustrate the synergistic influence of the NAO
 396 and ENSO on the persistence of SST anomalies (Table 2). Specifically, when the negative phase of
 397 NAO and ENSO occur together, the correlation coefficients between the NAOI and NATI are greater
 398 than those influenced by a single factor alone (Table 2).



399

400 **Figure 7.** Upper, correlation distributions of the (a) winter NAOI with winter SST, (b) winter NATI

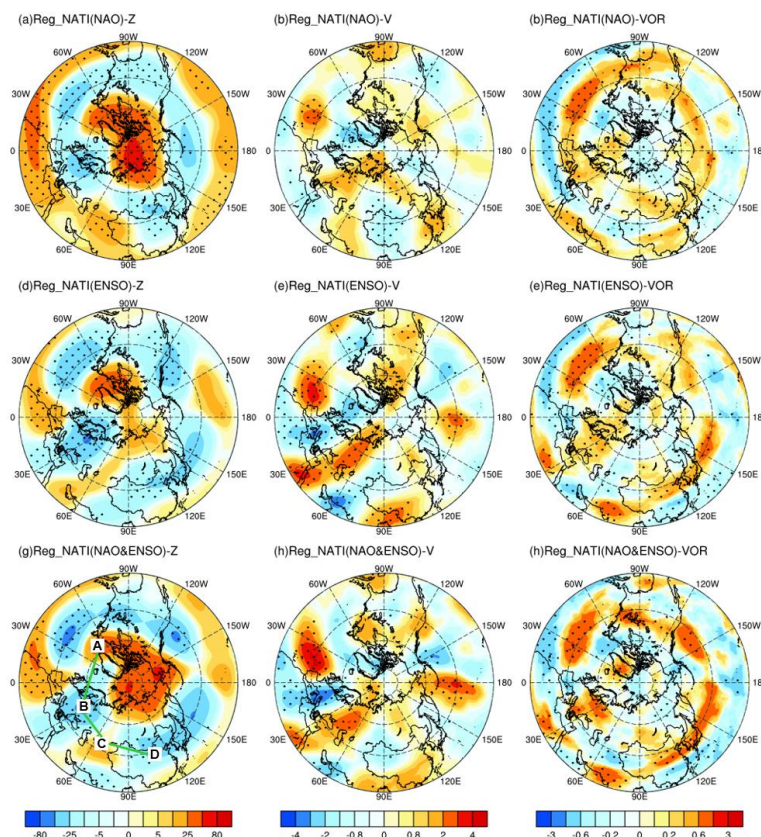


401 with spring SST, and (c) winter NATI with SST_p during negative NAO phases. Middle-Lower, as
 402 in the upper, but during the negative ENSO phases and concurrent negative phases of NAO and
 403 ENSO, respectively. Stippled areas are statistically significant at the 0.2 level.

404 **Table 2.** Correlation coefficients between the NAOI and NATI in three different categories. *
 405 indicates significant at the 0.1 level.

	DJF_NAO & DJF_NATI	DJF_NATI & MAM_NATI
NAO ⁻ phase	0.41*	0.51*
ENSO ⁻ phase	0.52*	0.69*
NAO ⁻ & ENSO ⁻ phase	0.66*	0.69*

406 The NAO preserves its anomalous signal within the tripole SST during the previous winter,
 407 and releases the signal in the following spring. Given the distance across the entire Eurasian
 408 continent between the North Atlantic and North China, the role of teleconnection wave trains is
 409 particularly important in influencing dust activities over North China. Figure 8a illustrates the
 410 geopotential height field at 200 hPa regressed onto the spring NATI during the negative phase of
 411 NAO. This reveals a pronounced north-south reversed dipole pattern in the North Atlantic, i.e.,
 412 negative over Azores and positive over Iceland, representing a typical negative NAO structure (e.g.,
 413 Wallace and Gutzler, 1981; Hurrell, 1995; Li and Wang, 2003). Meanwhile, a positive-negative-
 414 positive teleconnection wave train structure centered around eastern Europe, Middle East, and North
 415 China is observed, suggesting that the disturbance energy propagates downstream from the North
 416 Atlantic through waveguide effects, leading to an anticyclonic circulation anomaly in North China.
 417 Similar teleconnection wave-train propagation characteristics are also observed in the 200 hPa
 418 meridional wind and vorticity fields (Figure 8b, c). During the negative phase of ENSO, modulated
 419 by the NATI, analogous teleconnection structures are also seen in the circulation field (Figure 8d-
 420 f). Notably, when the NAO and ENSO are both in their negative phases, the teleconnection structure
 421 reflected in the circulation field is more pronounced than when only one factor is dominated (Figure
 422 8g-i), confirming the synergistic effects of both factors on the circulation processes affecting dust
 423 activities in North China.



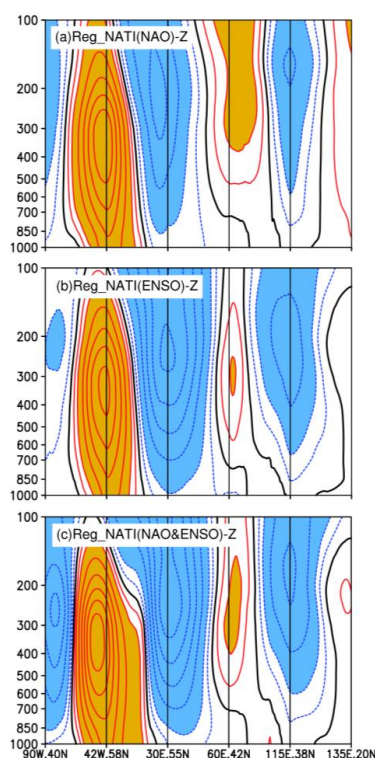
424

425 **Figure 8.** Upper, regression distribution of spring NATI against the spring (a) geopotential height
 426 (unit: gpm), (b) meridional wind (unit: $\text{m}\cdot\text{s}^{-1}$), and (c) vorticity (unit: $10^{-5}\cdot\text{m}\cdot\text{s}^{-1}$) at 200 hPa during
 427 the negative NAO phase. Middle-lower, as in the upper, but during the negative ENSO phases and
 428 concurrent negative phases of NAO and ENSO, respectively. Regression fields multiplied by -1.
 429 Stippled areas are statistically significant at the 0.2 level.

430 In order to further examine the impact mechanisms of the NAO and ENSO on the spring dust
 431 activities in North China, based on the propagation characteristics of the teleconnection wave train
 432 shown in Figure 8, the distribution of cross-section of the geopotential height field is presented
 433 (Figure 9). When both the NAO and ENSO are in their negative phases, the NATI anomalies
 434 correspond to the teleconnection wave train extending from the upper to lower troposphere, which
 435 is specifically characterized by a positive-negative-positive tripole pattern. This wave train
 436 propagates from the North Atlantic, traversing eastern Europe and Middle East, and ultimately
 437 influencing circulation processes associated with the dust weather over North China. Furthermore,
 438 the analysis of cross-section at different levels of the troposphere reveals that under the negative



439 phases of NAO and ENSO, the teleconnection wave train excited by the NATI exhibits quasi-
440 barotropic features, with this anomalous structure being primarily concentrated in the middle-upper
441 troposphere. When the NAO and ENSO are simultaneously in their negative phases, the intensity
442 and scope of the teleconnection wave train are significantly enhanced and expanded compared to
443 the influence of a single factor (Figure 9c), demonstrating synergistic effects.



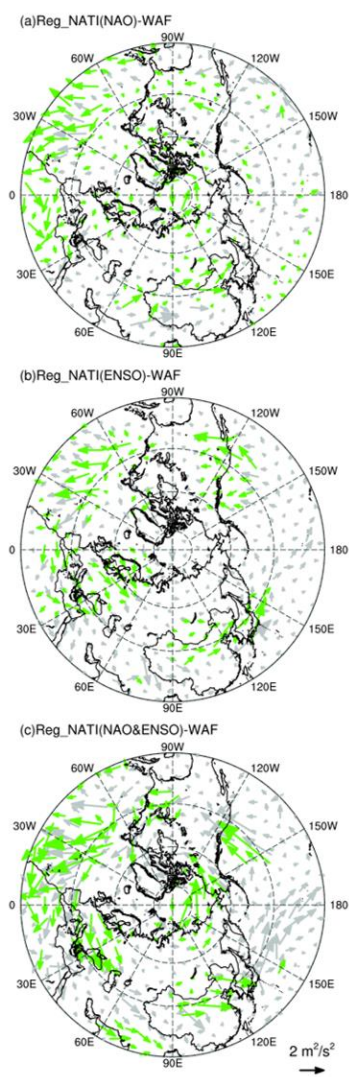
444

445 **Figure 9.** Vertical section of regression of spring NATI against the geopotential height along the
446 solid line labeled A (42°W, 58°N), B (30°E, 55°N), C (60°E, 42°N), and D (115°E, 38°N) in Figure
447 8g for (a) negative NAO phase in the previous winter. Panels (b)-(c) as in (a), but during the negative
448 ENSO phases and concurrent negative phases of NAO and ENSO, respectively (unit: gpm).
449 Regression fields have multiplied by -1. Shading indicates the absolute value is greater than 10 gpm.

450 To provide a more comprehensive analysis of the transport process of disturbance energy in
451 the atmosphere, the horizontal distribution of the WAF associated with spring NATI variations is
452 further examined. Under the scenario that either the NAO or ENSO is in their negative phases, WAF
453 can be clearly observed to originate from the North Atlantic, traverse the Eurasian continent, and
454 extend to the North China (Figures 10a-b). When both factors occur simultaneously, not only is the
455 transport intensity of WAF enhanced, but its impact range on the dust weather in North China is also



456 broadened (Figure 10c). Through the analysis of teleconnection wave trains and WAF, it is
457 determined that the synergistic effects not only enhance the disturbance intensity in the atmosphere
458 but also expand impact range, thereby promoting the occurrence and development of spring dust
459 weather in North China. The enhancement and expansion of atmospheric disturbances may be
460 related to large-scale circulation anomalies and local climate condition changes induced by the
461 synergistic effects of the NAO and ENSO, which in turn affect the transport and deposition
462 processes of dust.



463

464 **Figure 10.** Upper, regression distribution of spring NATI against the T-N wave activity flux (a)
465 during negative NAO phase. Middle-lower, as in upper, but during the negative ENSO phases and



466 concurrent negative phases of NAO and ENSO, respectively (units: $m^2 \cdot s^{-2}$). Regression fields have
467 multiplied by -1. Green arrows are statistically significant at the 0.2 level.

468 **4. Conclusions and discussions**

469 The NAO and ENSO exert significant impacts on climate variability in China (e.g., Zhang et
470 al., 2016; Wang et al., 2018; Feng et al., 2020). Although North China is not the primary dust source,
471 dusty disasters are notably active in this region during spring. This study highlights that the previous
472 winter NAO and ENSO exert essential influences on the following spring dust activities in North
473 China. Their impacts are asymmetric, manifesting only when both are in their negative phases.
474 Furthermore, the results indicate that NAO and ENSO in the negative phase have synergistic effects
475 on the spring dust activities in North China, promoting dust activities and with greater impacts than
476 their sole effect.

477 Under the regulatory influence of the negative phases of NAO and ENSO, the atmospheric
478 circulation in the troposphere from the lower to upper layers exhibits anomalies, including variations
479 in the upper-level zonal winds, mid-latitude trough-ridge systems, circulation over the WNP, and
480 SH at the SLP. These variations promote the occurrence and development of dust weather in North
481 China. Simultaneously, accompanying anomalies in the atmospheric circulation pattern also affect
482 local meteorological factors, including humidity and precipitation, which in turn show impacts on
483 the dust activities in North China. Notably, when both the NAO and ENSO are in their negative
484 phases, synergistic effects occur, making the anomalies in atmospheric circulation from the lower
485 to upper layers, as well as variations in humidity and precipitation, more conducive to the occurrence
486 of dust events in North China. The impact of NAO on the underlying SST pattern is predominantly
487 observed during its negative phase, elucidating why the NAO significantly influences dust activities
488 in North China only during its negative phase. Furthermore, when both the NAO and ENSO
489 simultaneously manifest in their negative phases, the teleconnection wave trains and WAF
490 stimulated from the North Atlantic are more intense, thereby more effectively influencing dust
491 activities in North China, indicating the synergistic effects of the two variabilities on the dust
492 activities over North China.

493 In the process where the previous winter NAO and ENSO affect the following spring dust
494 activities in North China, the persistence of anomalous NAT over North Atlantic plays an important
495 role. The previous winter NAO stores its signal in the NAT (Czaja and Frankignoul, 2002; Wu et
496 al., 2009). Due to the persistence of SST, the anomalous NAT can last from winter to spring (e.g.,



497 Wu et al., 2012; Zhang et al., 2021a; Li et al., 2023). In spring, NAT regulates the circulation pattern
498 in North China through teleconnection wave trains, ultimately affecting the dust activities over
499 North China. The signal of previous winter ENSO can persist into spring, due to the persistence of
500 SST, and it affects the dust activities in North China through two pathways: i.e., directly influencing
501 the dust activities in North China by affecting the circulation anomalies over the WNP, and playing
502 a facilitating role in the process where the NAO excites NAT, thereby affecting the dust activities in
503 North China. This provides a plausible explanation why the previous winter NAO and ENSO exert
504 synergistic effects on the following spring dust activities in North China.

505 This study investigated the impacts of NAO and ENSO on the dust activities in North China
506 and the involved physical processes, indicating the one season ahead signals provide as the useful
507 predictors for the spring dust activities in North China. Future work will focus on developing a
508 forecast model using the NAO and ENSO as predictors and validating its prediction effectiveness.
509 Additionally, as previous studies have highlighted strong interdecadal variations are existed in both
510 NAO and ENSO (Woollings et al., 2015; Dieppois et al., 2021; Wang et al., 2023), it is of interest
511 to further detect whether the synergistic effects of NAO and ENSO on the dusty activity over North
512 China experience interdecadal variations. However, due to the availability of dataset, the potential
513 impacts of the interdecadal variability of the NAO and ENSO on dust activities have not been
514 discussed in this study. Simultaneously, as reported that the state-of-art models can reproduce the
515 individual impact of NAO and ENSO on the dust activities in North China (Ginoux et al., 2004;
516 Yang et al., 2022a), whether their synergistic effects on the dust weather could be well simulated,
517 requiring further researches. Additionally, previous studies have indicated that the variability of
518 ENSO is likely to intensify under the background of global warming (Cai et al., 2021). Therefore,
519 it is crucial to investigate the future changes in the NAO, as well as future change of its synergistic
520 effects with the ENSO on the dust weather, to better understand the plausible trends of future dust
521 activities in North China.

522

523 **Code and data availability.** The MERRA-2 dust aerosol concentrations dataset can be downloaded
524 from <https://disc.gsfc.nasa.gov/datasets?project=MERRA-2> (last access: 28 March 2024). The
525 atmospheric reanalysis datasets, including the wind field, geopotential height field, and sea level
526 pressure field can be downloaded from
527 <https://cds.climate.copernicus.eu/#!/search?text=ERA5&type=dataset> (last access: 28 March 2024).
528 Our results can be made available upon request. The oceanic reanalysis data can be downloaded



529 from <https://www.metoffice.gov.uk/hadobs/hadisst> (last access: 28 March 2024). Our results can be
530 made available upon request.

531

532 **Author contributions.** FLX and JF conceptualized and designed the research. FLX and JF
533 synthesized and analyzed the data. FLX, SW, YL, and JF produced the figures. FLX and SW
534 contributed to the datasets retrieval. All the authors discussed the results and wrote the paper.

535 **Competing interests.** The authors declare that they have no conflict of interest.

536

537 **Disclaimer.** Publisher's note: Copernicus Publications remains neutral with regard to jurisdictional
538 claims in published maps and institutional affiliations.

539

540 **Acknowledgements.** This work was jointly supported by the National Key Research and
541 Development Program of China (2023YFF0805100), the BNU-FGS Global Environmental Change
542 Program (No. 2023-GC-ZYTS-03), and the State Key Laboratory of Tropical Oceanography, South
543 China Sea Institute of Oceanology, Chinese Academy of Sciences (Project No. LTO2310).

544

545 **Financial support.** This work was jointly supported by the National Key Research and
546 Development Program of China (2023YFF0805100), the BNU-FGS Global Environmental Change
547 Program (No. 2023-GC-ZYTS-03), and the State Key Laboratory of Tropical Oceanography, South
548 China Sea Institute of Oceanology, Chinese Academy of Sciences (Project No. LTO2310).

549



550 References

- 551 Abid, M. A., Kucharski, F., Molteni, F., Kang, I.-S., Tompkins, A. M., and Almazroui, M.: Separating the Indian and
552 Pacific Ocean Impacts on the Euro-Atlantic Response to ENSO and Its Transition from Early to Late Winter, *J.*
553 *Climate*, 34, 1531–1548, <https://doi.org/10.1175/JCLI-D-20-0075.1>, 2021.
- 554 Achakulwisut, P., Shen, L., and Mickley, L. J.: What Controls Springtime Fine Dust Variability in the Western United
555 States? Investigating the 2002–2015 Increase in Fine Dust in the U.S. Southwest, *J. Geophys. Res.-Atmos.*, 122,
556 <https://doi.org/10.1002/2017JD027208>, 2017.
- 557 Ayarzagüena, B., Ineson, S., Dunstone, N. J., Baldwin, M. P., and Scaife, A. A.: Intraseasonal Effects of El Niño–
558 Southern Oscillation on North Atlantic Climate, *J. Climate*, 31, 8861–8873, [https://doi.org/10.1175/JCLI-D-18-
0097.1](https://doi.org/10.1175/JCLI-D-18-
559 0097.1), 2018.
- 560 Cai, W., Santoso, A., Collins, M., Dewitte, B., Karamperidou, C., Kug, J.-S., Lengaigne, M., McPhaden, M. J.,
561 Stuecker, M. F., Taschetto, A. S., Timmermann, A., Wu, L., Yeh, S.-W., Wang, G., Ng, B., Jia, F., Yang, Y., Ying,
562 J., Zheng, X.-T., Bayr, T., Brown, J. R., Capotondi, A., Cobb, K. M., Gan, B., Geng, T., Ham, Y.-G., Jin, F.-F.,
563 Jo, H.-S., Li, X., Lin, X., McGregor, S., Park, J.-H., Stein, K., Yang, K., Zhang, L., and Zhong, W.: Changing
564 El Niño–Southern Oscillation in a warming climate, *Nat. Rev.-Earth Environ.*, 2, 628–644,
565 <https://doi.org/10.1038/s43017-021-00199-z>, 2021.
- 566 Chen, S., Zhao, D., Huang, J., He, J., Chen, Y., Chen, J., Bi, H., Lou, G., Du, S., Zhang, Y., and Yang, F.: Mongolia
567 Contributed More than 42% of the Dust Concentrations in Northern China in March and April 2023, *Adv. Atmos.*
568 *Sci.*, 40, 1549–1557, <https://doi.org/10.1007/s00376-023-3062-1>, 2023.
- 569 Csavina, J., Field, J., Félix, O., Corral-Avitia, A. Y., Sáez, A. E., and Betterton, E. A.: Effect of wind speed and
570 relative humidity on atmospheric dust concentrations in semi-arid climates, *Sci. Total Environ.*, 487, 82–90,
571 <https://doi.org/10.1016/j.scitotenv.2014.03.138>, 2014.
- 572 Czaja, A. and Frankignoul, C.: Observed Impact of Atlantic SST Anomalies on the North Atlantic Oscillation, *J.*
573 *Climate*, 15, 606–623, [https://doi.org/10.1175/1520-0442\(2002\)015<0606:OIOASA>2.0.CO;2](https://doi.org/10.1175/1520-0442(2002)015<0606:OIOASA>2.0.CO;2), 2002.
- 574 Dieppoiss, B., Capotondi, A., Pohl, B., Chun, K. P., Monerie, P.-A., and Eden, J.: ENSO diversity shows robust
575 decadal variations that must be captured for accurate future projections, *Communications Earth & Environment*,
576 2, 212, <https://doi.org/10.1038/s43247-021-00285-6>, 2021.
- 577 Ding, R., Nnamchi, H. C., Yu, J.-Y., Li, T., Sun, C., Li, J., Tseng, Y., Li, X., Xie, F., Feng, J., Ji, K., and Li, X.: North
578 Atlantic oscillation controls multidecadal changes in the North Tropical Atlantic–Pacific connection, *Nat.*
579 *Commun.*, 14, 862, <https://doi.org/10.1038/s41467-023-36564-3>, 2023.
- 580 Fan, K., Xie, Z., Wang, H., Xu, Z., and Liu, J.: Frequency of spring dust weather in North China linked to sea ice
581 variability in the Barents Sea, *Clim. Dyn.*, 51, 4439–4450, <https://doi.org/10.1007/s00382-016-3515-7>, 2018.
- 582 Feldstein, S. B.: The dynamics of NAO teleconnection pattern growth and decay, *Q. J. Roy. Meteor. Soc.*, 129, 901–
583 924, <https://doi.org/10.1256/qj.02.76>, 2003.
- 584 Feng, J. and Li, J.: Influence of El Niño Modoki on spring rainfall over south China, *J. Geophys. Res.-Atmos.*, 116,
585 D13102, <https://doi.org/10.1029/2010JD015160>, 2011.
- 586 Feng, J., Li, J., Liao, H., and Zhu, J.: Simulated coordinated impacts of the previous autumn North Atlantic
587 Oscillation (NAO) and winter El Niño on winter aerosol concentrations over eastern China, *Atmos. Chem.*
588 *Phys.*, 19, 10787–10800, <https://doi.org/10.5194/acp-19-10787-2019>, 2019.
- 589 Feng, J., Zhu, J., Li, J., and Liao, H.: Aerosol concentrations variability over China: two distinct leading modes,
590 *Atmos. Chem. Phys.*, 20, 9883–9893, <https://doi.org/10.5194/acp-20-9883-2020>, 2020.
- 591 Gelaro, R., McCarty, W., Suárez, M. J., Todling, R., Molod, A., Takacs, L., Randles, C. A., Darnenov, A., Bosilovich,
592 M. G., Reichle, R., Wargan, K., Coy, L., Cullather, R., Draper, C., Akella, S., Buchard, V., Conaty, A., Da Silva,



- 593 A. M., Gu, W., Kim, G.-K., Koster, R., Lucchesi, R., Merkova, D., Nielsen, J. E., Partyka, G., Pawson, S.,
594 Putman, W., Rienecker, M., Schubert, S. D., Sienkiewicz, M., and Zhao, B.: The Modern-Era Retrospective
595 Analysis for Research and Applications, Version 2 (MERRA-2), *J. Climate*, 30, 5419–5454,
596 <https://doi.org/10.1175/JCLI-D-16-0758.1>, 2017.
- 597 Ginoux, P., Prospero, J., Torres, O., and Chin, M.: Long-term simulation of global dust distribution with the
598 GOCART model: correlation with North Atlantic Oscillation, *Environ. Modell. Softw.*, 19, 113–128,
599 [https://doi.org/10.1016/S1364-8152\(03\)00114-2](https://doi.org/10.1016/S1364-8152(03)00114-2), 2004.
- 600 Gong, S. L., Zhang, X. Y., Zhao, T. L., Zhang, X. B., Barrie, L. A., McKendry, I. G., and Zhao, C. S.: A Simulated
601 Climatology of Asian Dust Aerosol and Its Trans-Pacific Transport. Part II: Interannual Variability and Climate
602 Connections, *J. Climate*, 19, 104–122, <https://doi.org/10.1175/JCLI3606.1>, 2006.
- 603 Guo, Y., Li, J., and Li, Y.: A Time-Scale Decomposition Approach to Statistically Downscale Summer Rainfall over
604 North China, *J. Climate*, 25, 572–591, <https://doi.org/10.1175/JCLI-D-11-00014.1>, 2012.
- 605 Hersbach, H., Bell, B., Berrisford, P., Hirahara, S., Horányi, A., Muñoz-Sabater, J., Nicolas, J., Peubey, C., Radu, R.,
606 Schepers, D., Simmons, A., Soci, C., Abdalla, S., Abellan, X., Balsamo, G., Bechtold, P., Biavati, G., Bidlot, J.,
607 Bonavita, M., De Chiara, G., Dahlgren, P., Dee, D., Diamantakis, M., Dragani, R., Flemming, J., Forbes, R.,
608 Fuentes, M., Geer, A., Haimberger, L., Healy, S., Hogan, R. J., Hólm, E., Janisková, M., Keeley, S., Laloyaux,
609 P., Lopez, P., Lupu, C., Radnoti, G., De Rosnay, P., Rozum, I., Vamborg, F., Villaume, S., and Thépaut, J.: The
610 ERA5 global reanalysis, *Q. J. Roy. Meteor. Soc.*, 146, 1999–2049, <https://doi.org/10.1002/qj.3803>, 2020.
- 611 Hu, Z., Ma, Y., Jin, Q., Idrissa, N. F., Huang, J., and Dong, W.: Attribution of the March 2021 exceptional dust storm
612 in North China, *B. Am. Meteorol. Soc.*, 104, E749–E755, <https://doi.org/10.1175/BAMS-D-22-0151.1>, 2023.
- 613 Huang, J., Li, Y., Fu, C., Chen, F., Fu, Q., Dai, A., Shinoda, M., Ma, Z., Guo, W., Li, Z., Zhang, L., Liu, Y., Yu, H.,
614 He, Y., Xie, Y., Guan, X., Ji, M., Lin, L., Wang, S., Yan, H., and Wang, G.: Dryland climate change: Recent
615 progress and challenges, *Rev. Geophys.*, 55, 719–778, <https://doi.org/10.1002/2016RG000550>, 2017.
- 616 Huang, J. P., Liu, J. J., Chen, B., and Nasiri, S. L.: Detection of anthropogenic dust using CALIPSO lidar
617 measurements, *Atmos. Chem. Phys.*, 15, 11653–11665, <https://doi.org/10.5194/acp-15-11653-2015>, 2015.
- 618 Huang, Y., Liu, X., Yin, Z., and An, Z.: Global Impact of ENSO on Dust Activities with Emphasis on the Key Region
619 from the Arabian Peninsula to Central Asia, *J. Geophys. Res.-Atmos.*, 126, e2020JD034068,
620 <https://doi.org/10.1029/2020JD034068>, 2021.
- 621 Hurrell, J. W.: Decadal Trends in the North Atlantic Oscillation: Regional Temperatures and Precipitation, *Science*,
622 269, 676–679, <https://doi.org/10.1126/science.269.5224.676>, 1995.
- 623 Ji, L. and Fan, K.: Climate prediction of dust weather frequency over northern China based on sea-ice cover and
624 vegetation variability, *Clim. Dyn.*, 53, 687–705, <https://doi.org/10.1007/s00382-018-04608-w>, 2019.
- 625 Jia, X. J., Derome, J., and Lin, H.: Comparison of the Life Cycles of the NAO Using Different Definitions, *J. Climate*,
626 20, 5992–6011, <https://doi.org/10.1175/2007JCLI1408.1>, 2007.
- 627 Jiang, W., Huang, G., Huang, P., Wu, R., Hu, K., and Chen, W.: Northwest Pacific Anticyclonic Anomalies during
628 Post-El Niño Summers Determined by the Pace of El Niño Decay, *J. Climate*, 32, 3487–3503,
629 <https://doi.org/10.1175/JCLI-D-18-0793.1>, 2019.
- 630 Jiménez-Esteve, B. and Domeisen, D. I. V.: The Tropospheric Pathway of the ENSO–North Atlantic Teleconnection,
631 *J. Climate*, 31, 4563–4584, <https://doi.org/10.1175/JCLI-D-17-0716.1>, 2018.
- 632 Ke, M., Wang, Z., Pan, W., Luo, H., Yang, S., and Guo, R.: Extremely Strong Western Pacific Subtropical High in
633 May 2021 Following a La Niña Event: Role of the Persistent Convective Forcing over the Indian Ocean, *Asia-
634 pac. J. Atmos. Sci.*, 59, 47–58, <https://doi.org/10.1007/s13143-022-00300-6>, 2023.
- 635 Kim, H. and Choi, M.: Impact of soil moisture on dust outbreaks in East Asia: Using satellite and assimilation data,
636 *Geophys. Res. Lett.*, 42, 2789–2796, <https://doi.org/10.1002/2015GL063325>, 2015.



- 637 Kim, S. and Kug, J.: What Controls ENSO Teleconnection to East Asia? Role of Western North Pacific Precipitation
638 in ENSO Teleconnection to East Asia, *J. Geophys. Res.-Atmos.*, 123, <https://doi.org/10.1029/2018JD028935>,
639 2018.
- 640 Kok, J. F., Storelvmo, T., Karydis, V. A., Adebisi, A. A., Mahowald, N. M., Evan, A. T., He, C., and Leung, D. M.:
641 Mineral dust aerosol impacts on global climate and climate change, *Nat. Rev.-Earth Environ.*, 4, 71–86,
642 <https://doi.org/10.1038/s43017-022-00379-5>, 2023.
- 643 Kueh, M.-T., Lin, C.-Y., and Chien, Y.-Y.: Temporal coherence in particulate matter in East Asian outflow regions:
644 fingerprints of ENSO and Asian dust, *npj Climate and Atmospheric Science*, 6, 201,
645 <https://doi.org/10.1038/s41612-023-00530-z>, 2023.
- 646 Li, J. and Wang, J. X. L.: A new North Atlantic Oscillation index and its variability, *Adv. Atmos. Sci.*, 20, 661–676,
647 <https://doi.org/10.1007/BF02915394>, 2003.
- 648 Li, J., Zheng, F., Sun, C., Feng, J., and Wang, J.: Pathways of Influence of the Northern Hemisphere Mid-high
649 Latitudes on East Asian Climate: A Review, *Adv. Atmos. Sci.*, 36, 902–921, [https://doi.org/10.1007/s00376-](https://doi.org/10.1007/s00376-019-8236-5)
650 019-8236-5, 2019.
- 651 Li, J., Carlson, B. E., Yung, Y. L., Lv, D., Hansen, J., Penner, J. E., Liao, H., Ramaswamy, V., Kahn, R. A., Zhang,
652 P., Dubovik, O., Ding, A., Laciš, A. A., Zhang, L., and Dong, Y.: Scattering and absorbing aerosols in the climate
653 system, *Nat. Rev.-Earth Environ.*, 3, 363–379, <https://doi.org/10.1038/s43017-022-00296-7>, 2022.
- 654 Li, Y., Xu, F., Feng, J., Du, M., Song, W., Li, C., and Zhao, W.: Influence of the previous North Atlantic Oscillation
655 (NAO) on the spring dust aerosols over North China, *Atmos. Chem. Phys.*, 23, 6021–6042,
656 <https://doi.org/10.5194/acp-23-6021-2023>, 2023.
- 657 Liu, J., Chen, J., Chen, S., Yan, X., Dong, H., and Chen, F.: Dust storms in northern China and their significance for
658 the concept of the Anthropocene, *Science China Earth Sciences*, 65, 921–933, [https://doi.org/10.1007/s11430-](https://doi.org/10.1007/s11430-021-9889-8)
659 021-9889-8, 2022.
- 660 Liu, X., Yin, Z., Zhang, X., and Yang, X.: Analyses of the spring dust storm frequency of northern China in relation
661 to antecedent and concurrent wind, precipitation, vegetation, and soil moisture conditions, *J. Geophys. Res.-*
662 *Atmos.*, 109, 2004JD004615, <https://doi.org/10.1029/2004JD004615>, 2004.
- 663 López-Parages, J., Rodríguez-Fonseca, B., and Terray, L.: A mechanism for the multidecadal modulation of ENSO
664 teleconnection with Europe, *Clim. Dyn.*, 45, 867–880, <https://doi.org/10.1007/s00382-014-2319-x>, 2015.
- 665 Lou, S., Russell, L. M., Yang, Y., Xu, L., Lamjiri, M. A., DeFlorio, M. J., Miller, A. J., Ghan, S. J., Liu, Y., and Singh,
666 B.: Impacts of the East Asian Monsoon on springtime dust concentrations over China, *J. Geophys. Res.-Atmos.*,
667 121, 8137–8152, <https://doi.org/10.1002/2016JD024758>, 2016.
- 668 Lou, S., Russell, L. M., Yang, Y., Liu, Y., Singh, B., and Ghan, S. J.: Impacts of interactive dust and its direct radiative
669 forcing on interannual variations of temperature and precipitation in winter over East Asia, *J. Geophys. Res.-*
670 *Atmos.*, 122, 8761–8780, <https://doi.org/10.1002/2017JD027267>, 2017.
- 671 McPhaden, M. J. and Zhang, X.: Asymmetry in zonal phase propagation of ENSO sea surface temperature anomalies,
672 *Geophys. Res. Lett.*, 36, 2009GL038774, <https://doi.org/10.1029/2009GL038774>, 2009.
- 673 Pan, L.: Observed positive feedback between the NAO and the North Atlantic SSTA tripole, *Geophys. Res. Lett.*, 32,
674 2005GL022427, <https://doi.org/10.1029/2005GL022427>, 2005.
- 675 Prospero, J. M., Nees, R. T., and Uematsu, M.: Deposition rate of particulate and dissolved aluminum derived from
676 saharan dust in precipitation at Miami, Florida, *J. Geophys. Res.-Atmos.*, 92, 14723–14731,
677 <https://doi.org/10.1029/JD092iD12p14723>, 1987.
- 678 Rayner, N. A., Parker, D. E., Horton, E. B., Folland, C. K., Alexander, L. V., Rowell, D. P., Kent, E. C., and Kaplan,
679 A.: Global analyses of sea surface temperature, sea ice, and night marine air temperature since the late



- 680 nineteenth century, *J. Geophys. Res.-Atmos.*, 108, 2002JD002670, <https://doi.org/10.1029/2002JD002670>,
681 2003.
- 682 Shao, T., Liu, Y., Tan, Z., Li, D., Luo, M., and Luo, R.: Characteristics and a mechanism of dust weather in Northern
683 China, *Clim. Dyn.*, 61, 1591–1606, <https://doi.org/10.1007/s00382-022-06644-z>, 2023.
- 684 Su, J., Zhang, R., Li, T., Rong, X., Kug, J.-S., and Hong, C.-C.: Causes of the El Niño and La Niña Amplitude
685 Asymmetry in the Equatorial Eastern Pacific, *J. Climate*, 23, 605–617, <https://doi.org/10.1175/2009JCLI2894.1>,
686 2010.
- 687 Sung, M., Lim, G., and Kug, J.: Phase asymmetric downstream development of the North Atlantic Oscillation and
688 its impact on the East Asian winter monsoon, *J. Geophys. Res.-Atmos.*, 115, 2009JD013153,
689 <https://doi.org/10.1029/2009JD013153>, 2010.
- 690 Takaya, K. and Nakamura, H.: A Formulation of a Phase-Independent Wave-Activity Flux for Stationary and
691 Migratory Quasigeostrophic Eddies on a Zonally Varying Basic Flow, *J. Atmospheric Sci.*, 58, 608–627,
692 [https://doi.org/10.1175/1520-0469\(2001\)058<0608:AFOAPI>2.0.CO;2](https://doi.org/10.1175/1520-0469(2001)058<0608:AFOAPI>2.0.CO;2), 2001.
- 693 Trenberth, K. E.: The Definition of El Niño, *B. Am. Meteorol. Soc.*, 78, 2771–2777, [https://doi.org/10.1175/1520-0477\(1997\)078<2771:TDOENO>2.0.CO;2](https://doi.org/10.1175/1520-0477(1997)078<2771:TDOENO>2.0.CO;2), 1997.
- 695 Wallace, J. M. and Gutzler, D. S.: Teleconnections in the Geopotential Height Field during the Northern Hemisphere
696 Winter, *Mon. Weather Rev.*, 109, 784–812, [https://doi.org/10.1175/1520-0493\(1981\)109<0784:TITGHF>2.0.CO;2](https://doi.org/10.1175/1520-0493(1981)109<0784:TITGHF>2.0.CO;2), 1981.
- 698 Wang, B., Wu, R., and Fu, X.: Pacific–East Asian Teleconnection: How Does ENSO Affect East Asian Climate?, *J.*
699 *Climate*, 13, 1517–1536, [https://doi.org/10.1175/1520-0442\(2000\)013<1517:PEATHD>2.0.CO;2](https://doi.org/10.1175/1520-0442(2000)013<1517:PEATHD>2.0.CO;2), 2000.
- 700 Wang, C., Ren, B., Li, G., Zheng, J., Jiang, L., and Xu, D.: An Interdecadal Change in the Influence of the NAO on
701 Atlantic-Induced Arctic Daily Warming around the Mid-1980s, *Adv. Atmos. Sci.*, 40, 1285–1297,
702 <https://doi.org/10.1007/s00376-022-2218-8>, 2023.
- 703 Wang, Z., Yang, S., Lau, N.-C., and Duan, A.: Teleconnection between Summer NAO and East China Rainfall
704 Variations: A Bridge Effect of the Tibetan Plateau, *J. Climate*, 31, 6433–6444, <https://doi.org/10.1175/JCLI-D-17-0413.1>, 2018.
- 706 Woollings, T., Franzke, C., Hodson, D. L. R., Dong, B., Barnes, E. A., Raible, C. C., and Pinto, J. G.: Contrasting
707 interannual and multidecadal NAO variability, *Clim. Dyn.*, 45, 539–556, <https://doi.org/10.1007/s00382-014-2237-y>, 2015.
- 709 Wu, B., Zhou, T., and Li, T.: Atmospheric Dynamic and Thermodynamic Processes Driving the Western North
710 Pacific Anomalous Anticyclone during El Niño. Part I: Maintenance Mechanisms, *J. Climate*, 30, 9621–9635,
711 <https://doi.org/10.1175/JCLI-D-16-0489.1>, 2017.
- 712 Wu, J., Kurosaki, Y., Shinoda, M., and Kai, K.: Regional Characteristics of Recent Dust Occurrence and Its
713 Controlling Factors in East Asia, *Sola*, 12, 187–191, <https://doi.org/10.2151/sola.2016-038>, 2016.
- 714 Wu, Z., Wang, B., Li, J., and Jin, F.: An empirical seasonal prediction model of the east Asian summer monsoon
715 using ENSO and NAO, *J. Geophys. Res.-Atmos.*, 114, 2009JD011733, <https://doi.org/10.1029/2009JD011733>,
716 2009.
- 717 Wu, Z., Li, J., Jiang, Z., He, J., and Zhu, X.: Possible effects of the North Atlantic Oscillation on the strengthening
718 relationship between the East Asian Summer monsoon and ENSO, *Int. J. Climatol.*, 32, 794–800,
719 <https://doi.org/10.1002/joc.2309>, 2012.
- 720 Xi, X. and Sokolik, I. N.: Dust interannual variability and trend in Central Asia from 2000 to 2014 and their climatic
721 linkages, *J. Geophys. Res.-Atmos.*, 120, <https://doi.org/10.1002/2015JD024092>, 2015.



- 722 Yang, Y., Zeng, L., Wang, H., Wang, P., and Liao, H.: Dust pollution in China affected by different spatial and
723 temporal types of El Niño, *Atmos. Chem. Phys.*, 22, 14489–14502, <https://doi.org/10.5194/acp-22-14489-2022>,
724 2022a.
- 725 Yang, Y., Li, M., Wang, H., Li, H., Wang, P., Li, K., Gao, M., and Liao, H.: ENSO modulation of summertime
726 tropospheric ozone over China, *Environ. Res. Lett.*, 17, 034020, <https://doi.org/10.1088/1748-9326/ac54cd>,
727 2022b.
- 728 Yao, W., Gui, K., Wang, Y., Che, H., and Zhang, X.: Identifying the dominant local factors of 2000–2019 changes in
729 dust loading over East Asia, *Sci. Total Environ.*, 777, 146064, <https://doi.org/10.1016/j.scitotenv.2021.146064>,
730 2021.
- 731 Yin, Z., Wan, Y., Zhang, Y., and Wang, H.: Why super sandstorm 2021 in North China? *Natl. Sci. Rev.*, 9, nwab165,
732 <https://doi.org/10.1093/nsr/nwab165>, 2021.
- 733 Yu, Y., Notaro, M., Liu, Z., Wang, F., Alkolibi, F., Fadda, E., and Bakhrjy, F.: Climatic controls on the interannual to
734 decadal variability in Saudi Arabian dust activity: Toward the development of a seasonal dust prediction model,
735 *J. Geophys. Res.-Atmos.*, 120, 1739–1758, <https://doi.org/10.1002/2014JD022611>, 2015.
- 736 Zhang, P., Wu, Z., and Jin, R.: How can the winter North Atlantic Oscillation influence the early summer
737 precipitation in Northeast Asia: effect of the Arctic sea ice, *Clim. Dyn.*, 56, 1989–2005,
738 <https://doi.org/10.1007/s00382-020-05570-2>, 2021a.
- 739 Zhang, R., Li, T., Wen, M., and Liu, L.: Role of intraseasonal oscillation in asymmetric impacts of El Niño and La
740 Niña on the rainfall over southern China in boreal winter, *Clim. Dyn.*, 45, 559–567,
741 <https://doi.org/10.1007/s00382-014-2207-4>, 2015.
- 742 Zhang, R., Tian, W., He, X., Qie, K., Liu, D., and Tian, H.: Enhanced influence of ENSO on winter precipitation
743 over southern China in recent decades, *J. Climate*, 1–36, <https://doi.org/10.1175/JCLI-D-21-0182.1>, 2021b.
- 744 Zhang, W., Li, J., and Jin, F.: Spatial and temporal features of ENSO meridional scales, *Geophys. Res. Lett.*, 36,
745 2009GL038672, <https://doi.org/10.1029/2009GL038672>, 2009.
- 746 Zhang, W., Li, H., Stuecker, M. F., Jin, F.-F., and Turner, A. G.: A New Understanding of El Niño’s Impact over East
747 Asia: Dominance of the ENSO Combination Mode, *J. Climate*, 29, 4347–4359, <https://doi.org/10.1175/JCLI-D-15-0104.1>, 2016.
- 749 Zhang, X. Y., Gong, S. L., Zhao, T. L., Arimoto, R., Wang, Y. Q., and Zhou, Z. J.: Sources of Asian dust and role of
750 climate change versus desertification in Asian dust emission, *Geophys. Res. Lett.*, 30, 2003GL018206,
751 <https://doi.org/10.1029/2003GL018206>, 2003.
- 752 Zhao, C., Yang, Y., Fan, H., Huang, J., Fu, Y., Zhang, X., Kang, S., Cong, Z., Letu, H., and Menenti, M.: Aerosol
753 characteristics and impacts on weather and climate over the Tibetan Plateau, *Natl. Sci. Rev.*, 7, 492–495,
754 <https://doi.org/10.1093/nsr/nwz184>, 2020.
- 755 Zhao, S., Li, J., and Sun, C.: Decadal variability in the occurrence of wintertime haze in central eastern China tied
756 to the Pacific Decadal Oscillation, *Sci. Rep.*, 6, 27424, <https://doi.org/10.1038/srep27424>, 2016.
- 757 Zhao, Y., Huang, A., Zhu, X., Zhou, Y., and Huang, Y.: The impact of the winter North Atlantic Oscillation on the
758 frequency of spring dust storms over Tarim Basin in northwest China in the past half-century, *Environ. Res.*
759 *Lett.*, 8, 024026, <https://doi.org/10.1088/1748-9326/8/2/024026>, 2013.
- 760 Zheng, F., Li, J., Li, Y., Zhao, S., and Deng, D.: Influence of the Summer NAO on the Spring-NAO-Based
761 Predictability of the East Asian Summer Monsoon, *J. Appl. Meteorol. Clim.*, 55, 1459–1476,
762 <https://doi.org/10.1175/JAMC-D-15-0199.1>, 2016a.
- 763 Zheng, Y., Zhao, T., Che, H., Liu, Y., Han, Y., Liu, C., Xiong, J., Liu, J., and Zhou, Y.: A 20-year simulated
764 climatology of global dust aerosol deposition, *Sci. Total Environ.*, 557–558, 861–868,
765 <https://doi.org/10.1016/j.scitotenv.2016.03.086>, 2016b.



- 766 Zhou, F., Shi, J., Liu, M.-H., and Ren, H.-C.: Linkage between the NAO and Siberian high events on the intraseasonal
767 timescale, *Atmos. Res.*, 281, 106478, <https://doi.org/10.1016/j.atmosres.2022.106478>, 2023.
- 768 Zhu, C., Wang, B., and Qian, W.: Why do dust storms decrease in northern China concurrently with the recent global
769 warming? *Geophys. Res. Lett.*, 35, 2008GL034886, <https://doi.org/10.1029/2008GL034886>, 2008.
- 770 Zuo, J., Ren, H.-L., Li, W., and Wang, L.: Interdecadal Variations in the Relationship between the Winter North
771 Atlantic Oscillation and Temperature in South-Central China, *J. Climate*, 29, 7477–7493,
772 <https://doi.org/10.1175/JCLI-D-15-0873.1>, 2016.